A Method for Reducing Standby Losses by Vehicle Detection and Switching Control in a System Configuration for Multiple Vehicles in Dynamic Wireless Power Transfer

Kanta Kobayashi
Faculty of Science and Engeneering
Tokyo University of Science
Chiba, Japan
kobayashi.kanta22@gmail.com

Takehiro Imura
Faculty of Science and Engeneering
Tokyo University of Science
Chiba, Japan

Yoichi Hori
Faculty of Science and Engeneering
Tokyo University of Science
Chiba, Japan

***Abstract*— In Dynamic wireless power transfer, it is essential to detect vehicles and perform switching control of the transmission coils because applying power to the transmission coils when no vehicle is present causes standby losses. Existing systems for vehicle detection and switching control of the transmission coils in DWPT systems cannot handle multiple vehicles. In this paper, we propose an N-Legged-Converter system that can handle multiple vehicles by controlling the voltage of each transmission coil individually according to the presence or absence of vehicles by phase shifting, thereby reducing losses during standby. As a result, vehicle detection was achieved without additional sensors, reducing standby losses by 99% in simulations and 96% in experiments.**

Keywords*— *Dynamic Wireless Power Transfer, Magnetic Resonance Coupling, Standby Losses, N-Legged-Converter component, formatting, style, styling, insert* (*key words)

I. Introduction

EVs are being promoted to achieve carbon neutrality. However, problems such as the high cost of batteries and long recharging times are hindering the widespread use of EVs. In order to solve these problems, Dynamic Wireless Power Transfer (DWPT), which supplies power while the vehicle is in motion, has been studied[1].

To realize DWPT in society, it is essential to have a system that can support multiple vehicles and vehicle types. This system must be able to operate differently for multiple transmission coils. However, the DWPT system currently under study, in which inverters are connected in parallel to a number of transmission coils, cannot handle the above case. This is due to the fact that the voltage applied to each transmission coil is equal.[2] To make an existing system compatible with the above case, it is possible to connect an inverter to each transmission coil on a one-to-one basis. However, inverters are very expensive, so an N-Legged-Converter (NLC) is used in this paper to reduce the cost[3][4].

Another problem is that if voltage is applied to the transmission coils even when vehicles are not present in existing systems, the magnitude of leakage magnetic field and standby loss becomes non-negligible. Therefore, it is necessary to switch the voltage applied to each transmission coil according to the presence or absence of a vehicle. To do so, the vehicle must be detected on the transmission side and the power transmission coil that transmits power and the power transmission, but if switching, etc. is performed with a switch, current will not flow in any of the multiple transmission coils except the coil that is transmitting power, making it impossible to rely on an additional sensor to detect the vehicle or to support multiple vehicles.[5],[6] Furthermore, in the circuit configuration of WPT, there are two methods: S-S and double-LCC, both of which are being investigated for dynamic wireless power transfer (DWPT) systems [7]-[11].There is a method to solve this problem by applying a smaller voltage through phase shifting[12], but it is impossible to support multiple vehicles because the inverter and the power transmission coils are connected one-to-one.

Therefore, this paper proposes a method to reduce standby loss by vehicle detection and switching control in a system configuration where DWPT can be applied to multiple transmission coils.

II. Ease of Use

A. Double-LCC topology

As transmission circuits for WPT, the S-S (Series-Series) method, in which a capacitor is connected in series with the power transmission coil, and the Double-LCC method, in which an LCL filter with gyrator characteristics is applied, have been proposed. The Double-LCC scheme used in this paper is designed so that the frequency f_0 of the power supply causes LC resonance at each closed circuit shown in Fig. 1, and the inductance and capacitance are assumed to satisfy the resonance condition in equation (1). The current I_{in} flowing in the LCC resonant circuit on the transmission side is shown in Equation (2).

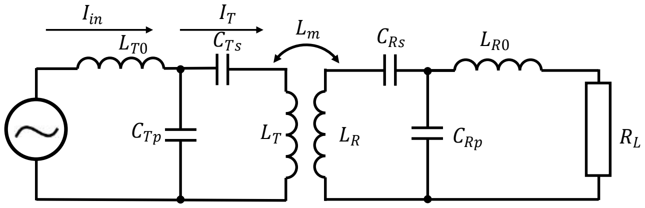

Fig.1 Double-LCC topology

$$f_0 = \frac{1}{2\pi\sqrt{L_{T0}C_{Tp}}} = \frac{1}{2\pi}\sqrt{\frac{C_{Tp}+C_{Ts}}{L_T C_{Tp} C_{Ts}}} = \frac{1}{2\pi\sqrt{L_{R0}C_{Rp}}} = \frac{1}{2\pi}\sqrt{\frac{C_{Rp}+C_{Rs}}{L_R C_{Rp} C_{Rs}}} \quad (1)$$

$$I_{in} = \frac{v_{in}k^2\omega^2 L_T L_R C_{Tp} C_{Rp} R_L}{L_{R0}\left(L_T - \frac{1}{\omega^2 C_{Ts}}\right)} \tag{2}$$

Equation (2) shows that in the double-LCC method, I_{in} increases in proportion to the coupling coefficient k between the transmitter and receiver sides, so that the vehicle can be detected by monitoring the change in I_{in}. Therefore, the vehicle can be detected using the transmission coil without the need for additional sensors.

In the S-S method, a large current flow when the vehicle is not on the transmission coil, which may cause damage to the circuit or power supply equipment if the switching control of the transmission coil is not performed or if a false detection occurs. However, in the Double-LCC method, when there is no coupling between the receiving k coil and the transmission coil, the input current I_{in} becomes 0 when the coupling coefficient is 0 from formula (2). Therefore, the Double-LCC method is superior to the S-S method in that voltage can be applied even when there is no coupling between the transmitter and receiver coils.

B. *N-Legged-Converter*

The N-Leg-Converter (NLC) used in this study is shown in Fig. 2. The NLC is an inverter consisting of n Legs connected in parallel to n-1 transmission coils. This greatly reduces the number of very expensive MOSFETs.

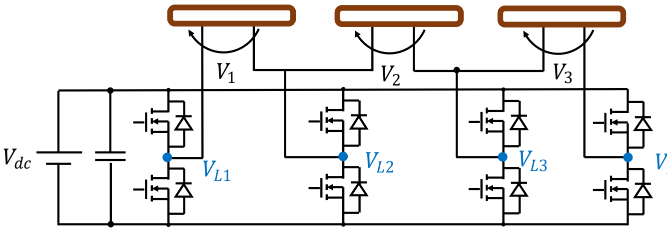

Fig.2 N-Legged Converter

Fig. 3 shows the potentials of two adjacent Legs, and Fig. 4 shows the voltage between the terminals of two adjacent Legs. If the phase of the i-th Leg is D_i, the phase difference between the i-th and i+1-th Legs is expressed as $\Delta D_i = D_{i+1} - D_i$.

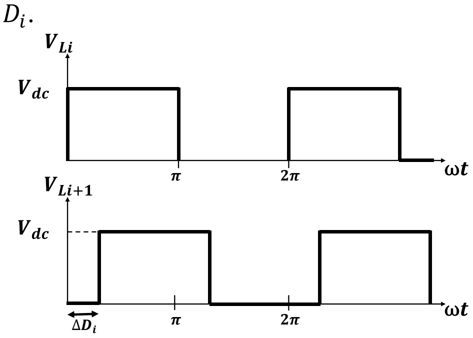

Fig.3 Voltagef adjacent Leg

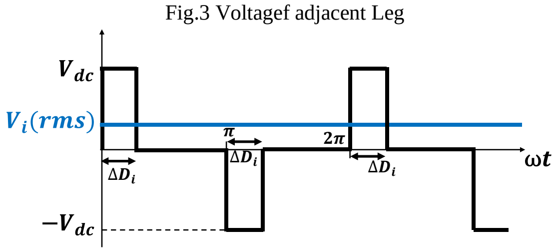

Fig.4 Voltage and phase of adjacent Leg

From ig.4, the RMS value of the voltage between the i-th and i+1-th Leg terminals is as follows (3).

$$V_i(rms) = \frac{2\sqrt{2}}{\pi} V_{dc} \sin\left(\frac{\Delta D_i}{2}\right) \tag{3}$$

Therefore, in NLC, the voltage applied to each transmission coil can be varied by changing the phase difference between adjacent Legs.

III. METHOD

A. *system configuration*

The proposed system is shown in Fig. 5. As described in 1. Introduction, an N-Legged-Converter was used in this paper to provide independent control for each transmission circuit.

For the resonant circuits, the Double-LCC method was used to detect vehicles using the transmission coils.

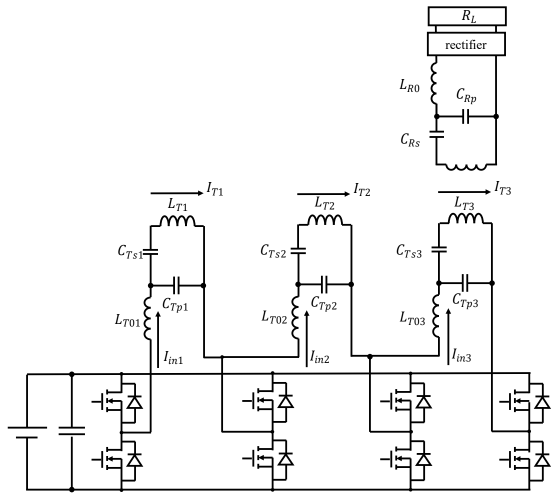

Fig.5 Primary circuit in the proposed method

B. *Flow of the proposed method*

Fig. 6 shows a specific control method. In this simulation, the system is set to standby with a phase difference of 3° and a small voltage applied to the transmission coils, and a vehicle is detected from the change in input current. Once a vehicle is detected, the control is performed by phase-shifting the phase difference between adjacent Legs to 180° so that the voltage applied to the corresponding transmission coil is maximized. In the experiment, the phase difference in standby mode was 20° because the experiment was conducted at low power due to hardware limitations.

Fig. 7 shows the control flowchart of the proposed system. Here, $I_{in,j}$ is the input current to the jth power transmission coil, and $Mode_j$ is the state of the jth power transmission coil, with transfer during power transmission. I_{th_low} and I_{th_high} are the threshold values of input current, respectively. When the input current exceeds I_{th_low}, it indicates that a vehicle is approaching, and when it falls below I_{th_high}, it indicates that a vehicle has passed by. D_w is the phase difference during standby, which in this paper is 3° during simulation and 20° during experiment.

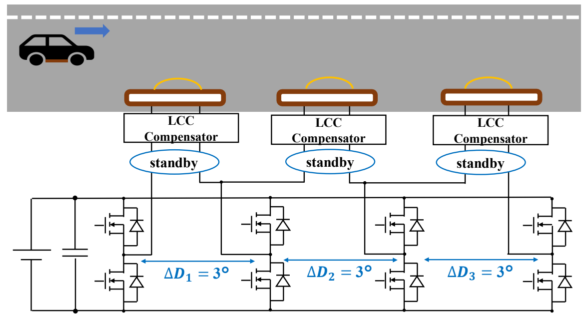

(a) Before vehicle entry

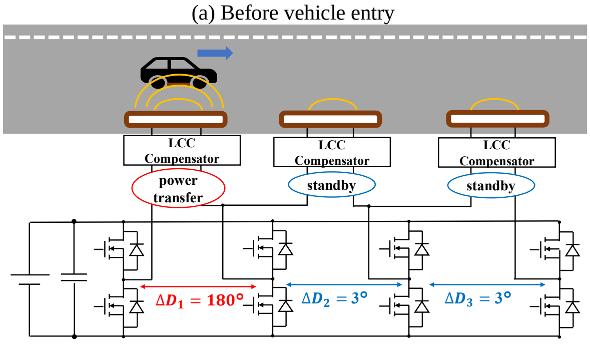

(b) Power transfer from the first transmission coil

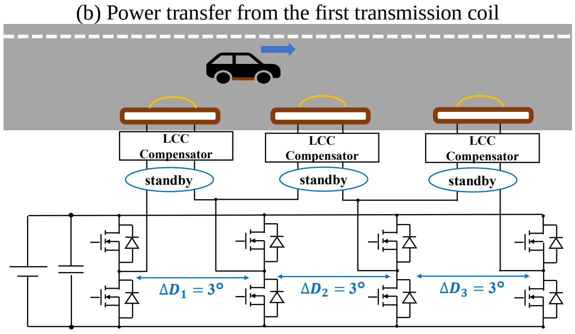

(c) Vehicle passes the first primary coil

Fig.6 Flow of the proposed method

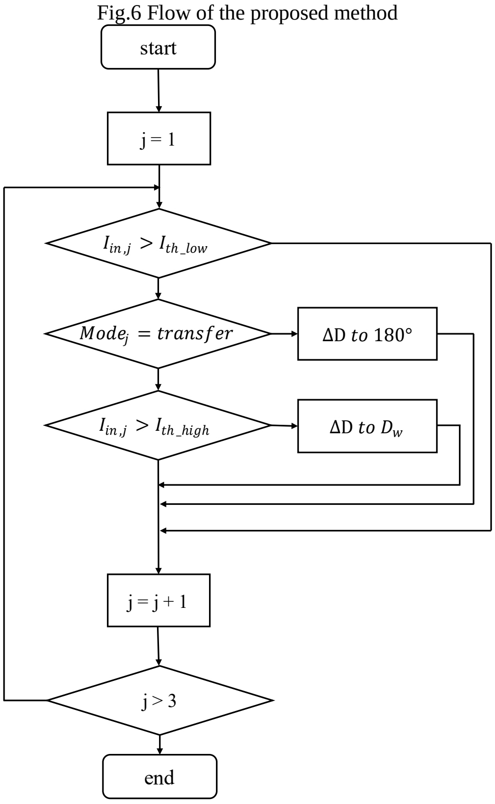

Fig.7 Flowchart of the proposed method

IV. Simulation Results

A. Method and sensitivity of vehicle detection

Fig. 8a shows the mutual inductance of one vehicle traveling at 60 km/h over three transmission coils, and Fig. 8b and c show the input currents from the NLC to the LCC circuit when all Legs of the NLC are operated with a phase difference of 180° and 3°, respectively, without vehicle detection or other control.

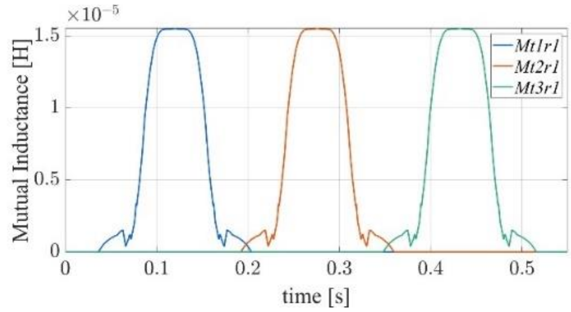

(a) mutual inductance

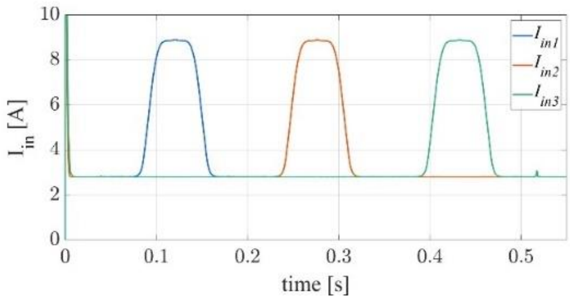

(b) Phase difference 180°

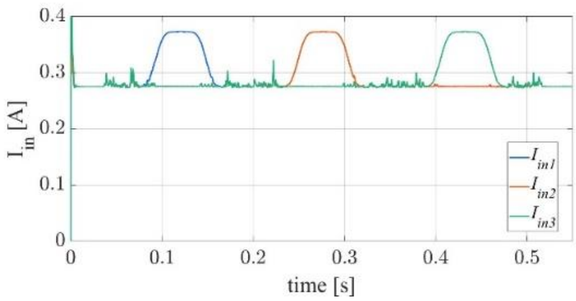

(c) Phase difference 3°

Fig.8 Comparison of DWPT with phase shifted by NLC.

Fig. 8 shows that the input current I_{in} from the NLC to the resonance circuit increases in proportion to the increase in mutual inductance due to the coupling between the transmission and receiving coils caused by the vehicle approaching the transmission coil, as shown in (a). This indicates that even if the voltage applied to the resonance circuit changes due to the phase shift of the NLC, the input current I_{in} is independent of the amount of phase shift, and the current value increases with the coupling between the transmitting and receiving coils. Therefore, even if the input current I_{in} is suppressed by the NLC phase shift in standby mode as in the proposed method, vehicle detection is still possible.

B. Simulation results of the proposed method

The purpose of this simulation is to demonstrate that the proposed method adequately performs detection and switching control when one vehicle travels at 60 km over three transmission coils. It is also to verify that the proposed method can operate at a power scale that is not possible in the experiment due to hardware limitations, and that it can handle multiple vehicles.

Fig. 9 shows the results of simulations conducted in MATLAB/Simulink based on the circuit configuration shown in Fig. 5. 3° and 180°, respectively.

The parameters during the simulation are shown in table1.

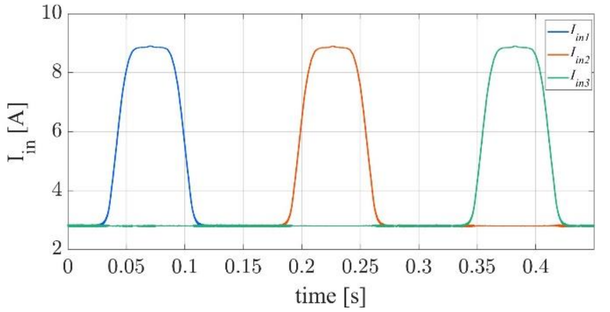

(a)Without control

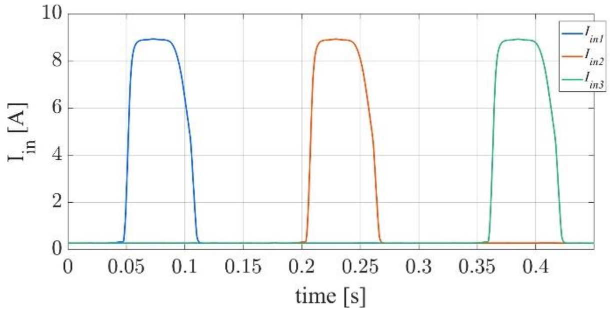

(b) Proposed Method

Fig9 Input current I_{in} from NLC to resonant circuit.

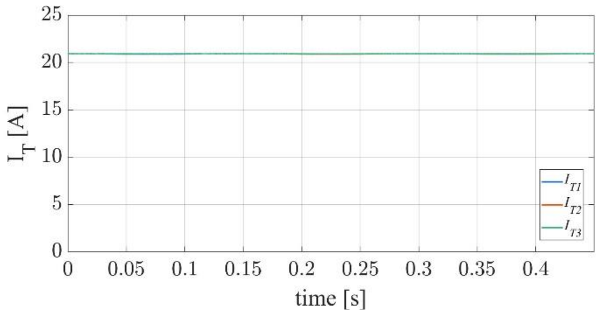

(a)Without control

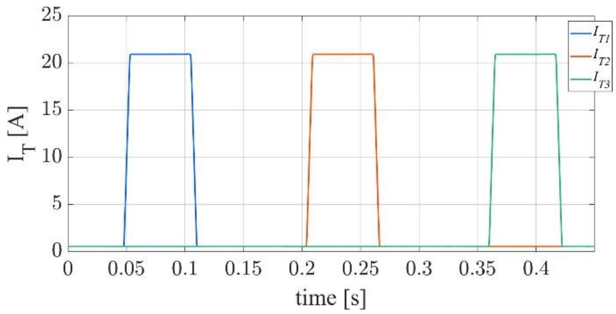

(b) Proposed Method

Fig.10 Current I_T flowing in the Primary coil.

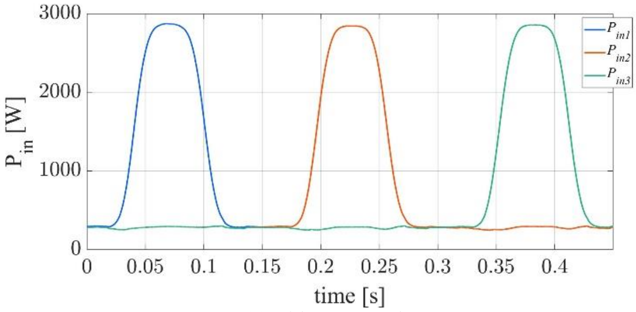

(a)Without control

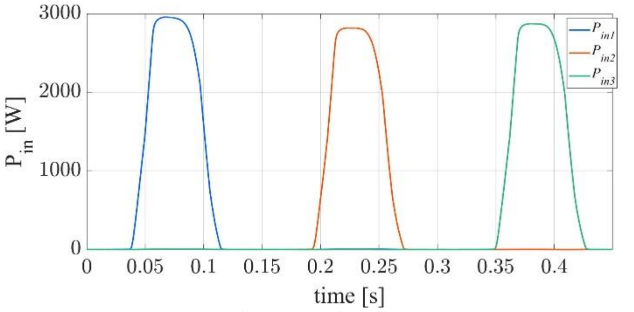

(b) Proposed Method

Fig.11 Input power P_{in} from NLC to resonant circuit.

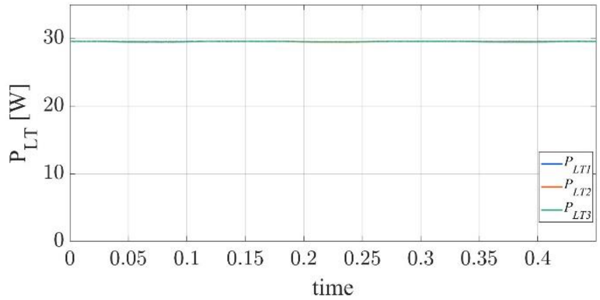

(a)Without control

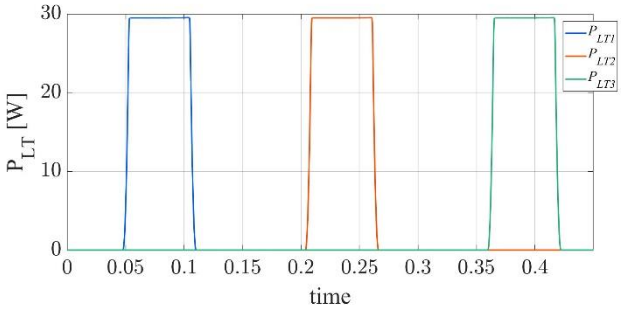

(b) Proposed Method

Fig.12 Power at the primary coil.

Table 1 Simulational parameters.

Vehicle velocity	V	60 km/h
Load voltage	V_{dc}	277.7 V
Operation frequency	f	85 kHz
Primary compensated inductance	L_{T0}	22.4 μH
Primary compensated capacitor	C_{Tp}	156.5 nF
Primary resonant capacitor	C_{Ts}	33.7 nF
Primary transmitter inductance	L_T	126.5 μH
Primary transmitter resistance	r_T	67.5 mΩ
Secondary compensated inductance	L_{R0}	42 μH
Secondary compensated capacitor	C_{Rp}	83.5 nF
Secondary resonant capacitor	C_{Rs}	30.9 nF
Secondary receiver inductance	L_R	155.6 μH
Secondary receiver resistance	r_R	22.8 mΩ
Secondary load resistance	R_L	45 Ω

According to Figures 9 and 10, the current without control is 20.9 A. However, with the proposed method, it decreases to 0.55 A, which is a reduction rate of 97.2%. These results confirm that the proposed method can reduce the current of all closed circuits in the power transmission system by 90% during standby. Figures 11 and 12 demonstrate that the proposed method can achieve a 99% reduction in input power to the power transmission system after NLC, resulting in a 99% reduction in standby loss. Moreover, the power consumption of the power transmission coils during standby can also be reduced by 99%, leading to a significant decrease in the heat generated by the coils. To demonstrate the feasibility of the proposed method, Figure 13 shows the simulation results of two vehicles with the same speed entering a single power transmission section. By using the proposed method, standby loss is reduced to about 3W, which is also a 99% reduction as in Figure 11. These results confirm that the proposed system can detect and switch power transmission coils even when multiple vehicles enter a single power transmission section.

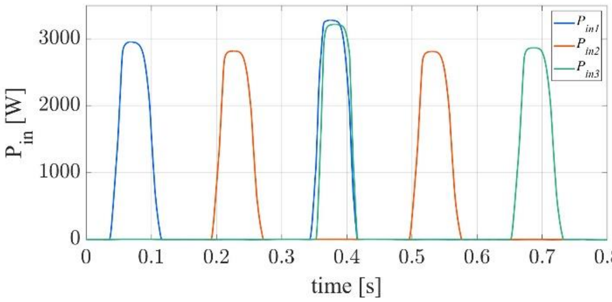

Fig.9 Input power P_{in} from NLC to resonant circuit in the detection of two vehicles.

V. Experiment Results

The experimental results are shown in Fig. 10, where the phase difference of the NLC is 180° for both standby and power transmission with no control, and 20° and 180° for standby and power transmission, respectively, with the proposed method. The parameters for the experiments are shown in Table 2 and Table3. Also, Fig. 10 shows the overview of experiment.

Table2 The primary-side parameters for an experiment.

		TX1	TX2	TX3
Input voltage	V_{in}	10 V	10 V	10 V
frequency	f	85 kHz	85 kHz	85 kHz
coil size		500 × 250 mm	500 × 250 mm	500 × 250 mm
Primary compensated inductance	L_0	49.40 µH	50.72 µH	50.63 µH
Primary compensated coil resistance	r_0	146.64 mΩ	150.49 mΩ	138.92 mΩ
Primary compensated capacitor	C_{1p}	70.33 nF	70.50 nF	70.98 nF
Primary resonant capacitor	C_{1s}	22.58 nF	22.49 nF	22.04 nF
Primary transmitter inductance	L_1	206.2 µH	206.3 µH	206.6 µH
Primary transmitter resistance	r_1	139.14 mΩ	138.57 mΩ	138.33 mΩ

Table3 The secondary-side parameters for an experiment.

Load resistance	R_L	300 Ω
coil size		250 × 250 mm
Secondary compensated inductance	L_0'	49.32 µH
Secondary compensated coil resistance	r_0'	143.33 mΩ
Secondary compensated capacitor	C_{2p}	70.93 nF
Secondary resonant capacitor	C_{2s}	56.0 nF
Secondary receiver inductance	L_2	112.38 µH
Secondary receiver resistance	r_2	86.73 mΩ

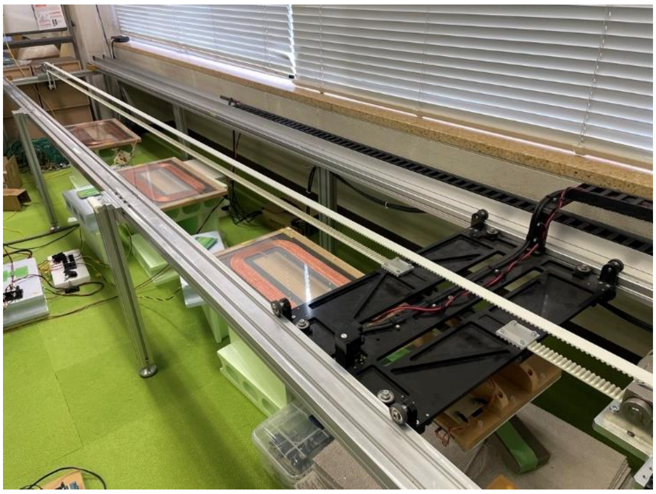

Fig. 10 shows the overview of experiment.

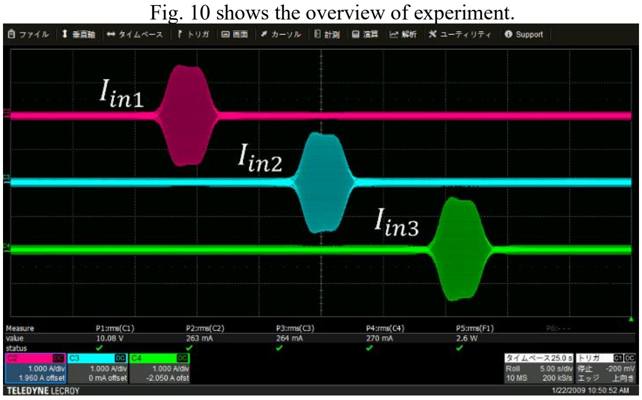

(a)Without control

(b) Proposed Method

Fig.11 Input current I_{in} from NLC to resonant circuit.

Fig. 11 shows the waveform of the current flowing from the inverter to each resonant circuit. It can be seen that the inverter is able to detect the receiving coil moving at 100 mm/s, switch the coil to transmit power, and perform power transmission.

(a) Phase difference 180 °

(b) Phase difference 20 °

Fig.12 Comparison of input voltage, input current, and current flowing in the transmission coil for different phase differences.

From Figure12, it can be seen that when the phase difference is 180°, the input voltage is 9.67V(RMS), the input current is 50.4mA(RMS), and the current flowing through the transmitting coil is 343mA(RMS). During standby, that is, when the phase difference is 20°, the input voltage is 3.20V(RMS), the input current is 25.8mA(RMS), and the current flowing through the transmitting coil is 64mA(RMS). Therefore, it is possible to reduce the input voltage by 66.9%, the input current by 48.8%, and the current flowing through the transmitting coil by 81.4% by setting the phase difference to 20° during standby. Furthermore, the input power when the phase difference is 180° is 109mW, while it is only 4mW during standby with a 20° phase difference. This reduction in input power indicates a 96.3% reduction in standby losses, confirming that using a 20° phase difference can significantly reduce standby losses.

VI. Conclusion

In this paper, the conventional inverter configuration is changed to NLC to make the system configuration capable of applying voltage to each transmission coil independently. In addition, we proposed a control method for vehicle detection and switching of the transmission coils by reducing the applied voltage through phase shifting with the NLC during standby, and verified it through simulation and experiment. The current flowing in the transmission coil during standby was reduced by 90% in the simulation and by nearly 50% in the experiment. Therefore, it was verified that the leakage magnetic field could be reduced and the standby loss could be reduced by 99% in the simulation and 96% in experiments. In addition, the simulation verified that the proposed method can handle the case where multiple vehicles enter the transmission section. The reason for the smaller reduction ratio in both simulation and experiment is thought to be that the phase difference between the standby and power transmission phases is 3° and 20°, respectively, which reduces the rate of decrease of the voltage applied to the resonance circuit during standby and power transmission. This is thought to be due to the fact that the input voltage can only be applied up to 10 V due to hardware limitations, which also limits the smallness of the phase difference.

Acknowledgment

This paper is based on results obtained from a project commissioned by Ministry of Land, Infrastructure, Transport and Tourism (MLIT) in Japan.

[1] C. Mi, G. Buja, S. Y. Choi, and C. T. Rim : “Modern Advances in Wireless Power Transfer Systems for Roadway Powered Electric Vehicles”, IEEE Transaction Industrial Electronics., Vol.63, No.10 pp.6533–6545 (2016)

[2] K. Song, C. Zhu, K. -E. Koh, D. Kobayashi, T. Imura and Y. Hori, "Modeling and design of dynamic wireless power transfer system for EV applications," *IECON 2015 - 41st Annual Conference of the IEEE Industrial Electronics Society*, Yokohama, Japan, 2015, pp. 005229-005234.

[3] F. Farajizadeh, M. Vilathgamuwa, P. Jayathurathnage and G. Ledwich, "Expandable N-Legged Converter for Dynamic Wireless Power Transfer," *2018 IEEE 18th International Power Electronics and Motion Control Conference (PEMC)*, Budapest, Hungary, 2018, pp. 115-120.

[4] F. Farajizadeh, D. M. Vilathgamuwa, D. Jovanovic, P. Jayathurathnage, G. Ledwich and U. Madawala, "Expandable N-Legged Converter to Drive Closely Spaced Multitransmitter Wireless Power Transfer Systems for Dynamic Charging," in *IEEE Transactions on Power Electronics*, vol. 35, no. 4, pp. 3794-3806, April 2020.

[5] J. L. Afonso, M. C. Martinez, L. A. Lisboa Cardoso and A. A. Nogueiras Meléndez, "RFID-triggered power activation for smart dynamic inductive wireless power transfer," *IECON 2017 - 43rd Annual Conference of the IEEE Industrial Electronics Society*, Beijing, China, 2017, pp. 6967-6973.

[6] D. Patil, J. M. Miller, B. Fahimi, P. T. Balsara and V. Galigekere, "A Coil Detection System for Dynamic Wireless Charging of Electric Vehicle," in *IEEE Transactions on Transportation Electrification*, vol. 5, no. 4, pp. 988-1003, Dec. 2019

[7] K. Tokita, K. Hata, H. Fujimoto and Y. Hori, "Sensorless Vehicle Detection Using Voltage Pulses with Envelope Model for In-motion Wireless Power Transfer System," *IECON 2019 - 45th Annual Conference of the IEEE Industrial Electronics Society*, Lisbon, Portugal, 2019, pp. 4329-4334

[8] K. Takeda and T. Koseki, "Improvement of Efficiency of Multi-Parallel Dynamic Wireless Power Transfer System with LCC Topology," *IECON 2018 - 44th Annual Conference of the IEEE Industrial Electronics Society*, Washington, DC, USA, 2018, pp. 4810-4815

[9] Kanta Sasaki and Takehiro Imura, "Combination of Sensorless Energized Section Switching System and Double-LCC for DWPT," 2020 IEEE PELS Workshop on Emerging Technologies; Wireless Power (WoW2020), Nov. 2020.

[10] Y. Yamada and T. Imura, "Maximum Output Power Design Considering the Efficiency in Wireless Power Transfer Coils," *IECON 2021 – 47th Annual Conference of the IEEE Industrial Electronics Society*, Toronto, ON, Canada, 2021, pp. 1-6

[11] Y. Yamada, S. Hasegawa, T. Imura and Y. Hori, "Design Method of Coreless Coil Considering Power, Efficiency and Magnetic Field Leakage in Wireless Power Transfer," the 48th Annual Conference of the IEEE Industrial Electronics Society (IES), IECON2022, Brussels, Belgium,Oct17-20,2022.

[12] H. Wang, U. Pratik, A. Jovicic, N. Hasan and Z. Pantic, "Dynamic Wireless Charging of Medium Power and Speed Electric Vehicle," in IEEE Transactions on Vehicular Technology, vol. 70, no. 12, pp. 12552-12566, Dec. 2021.